The Pyrolysis Behaviors of Polyimide Foam Derived from 3,3′,4,4′-Benzophenone Tetracarboxylic Dianhydride/4,4′-Oxydianiline

Yan-Xia Shen, Mao-Sheng Zhan, Kai Wang, Xiao-Huan Li, Pi-Chang Pan

School of Materials Science and Engineering, Beihang University, Beijing 100191, China

Received 19 November 2008; accepted 25 July 2009
DOI 10.1002/app.31189
Published online 7 October 2009 in Wiley InterScience (www.interscience.wiley.com).

ABSTRACT: The thermal stability and pyrolysis behaviors of polyimide (PI) foam derived from 3,3′,4,4′-benzophenone tetracarboxylic dianhydride (BTDA)/4,4′-oxydianiline (4,4′-ODA) in air and in nitrogen were studied. The decomposition products of PI foam were analyzed by thermogravimetry-Fourier transform infrared spectroscopy (TG-FTIR). Several integral and differential methods reported in the literatures were used in decomposition kinetics analysis of PI foam. The results indicated that the PI foam was easier to decompose in air than in nitrogen, with ~ 55% residue remaining in nitrogen versus zero in air at 800°C. The main pyrolysis products were CO_2, CO, and H_2O in air and CO_2, CO, H_2O, and small organic molecules in nitrogen. The different dynamic methods gave similar results that the apparent activation energies, pre-exponential factors, and reaction orders were higher in nitrogen than those in air. © 2009 Wiley Periodicals, Inc. J Appl Polym Sci 115: 1680–1687, 2010

Key words: polyimide foam; TG-FTIR; pyrolysis behavior; decomposition kinetics

INTRODUCTION

The common polymeric foams (polystyrene foam, polyurethane foam, polyethylene foam, phenolic foam, and so on) have been limited by their low service temperatures and susceptibility to degradation. The long-term service temperatures of most common polymeric foams are lower than 200°C, and 5% weight loss temperatures are lower than 450°C in air.[1–3] The long-time service temperatures of PI foams are higher than 200°C. The glass translation temperatures of some PI foams are higher than 300°C. Therefore, PI foam has been applied as thermal and acoustic insulation materials in the fields of aerospace and navigation, which may be due to its high and low temperature resistance, low smoke, low toxicity, low volatile, no halogen, no ozone consumption, easy installation, and so on.[4–8] But, PI foam will degrade rapidly at more than 500°C. In reusable launch vehicle (RLV) mission from launch to orbit and to reentry, the surface temperature of PI foam used as thermal protection system (TPS) will increase rapidly in short time and PI foam will degrade or fall off.[9] Therefore, studying the pyrolysis behaviors and products of PI foam is of both scientific significance and engineering applied importance.

At present, the researches on the pyrolysis behaviors and products of polyimide are still in progress.[10–18] Decomposition reaction order of polyimide is not the first order. And the main pyrolysis products of polyimide are CO, CO_2, and H_2O. The foaming agents and additives in PI foam perhaps have effect on pyrolysis behaviors and products. National aeronautics and space administration (NASA) investigated the effects of density, surface area, and chemical structure on flame retardancy properties of TEEK PI foam.[9,19,20] However, the pyrolysis behaviors and mechanisms of PI foams have not been studied. More quantitative parameters of thermal stability and degradation products of PI foam are needed for practical application.

In this article, the pyrolysis behaviors and products of PI foam derived from BTDA/4,4′-ODA in air and in nitrogen were studied by thermogravimetry-differential thermogravimetry (TG-DTG) and TG-FTIR. Thermal stability and environment-friendly program of PI foam were evaluated. These results provided reference data for practical application. The kinetics parameters were calculated by integral, differential, and special methods. The pyrolysis studies of polyimide foam gave insight into the parameters most important to the performance of this material for insulation and fire resistant structural components on future vehicles.

Correspondence to: M.-S. Zhan (zhanms@buaa.edu.cn).
Contract grant sponsor: National Science Council of the Republic of China; contract grant number: 2006AA03Z56.

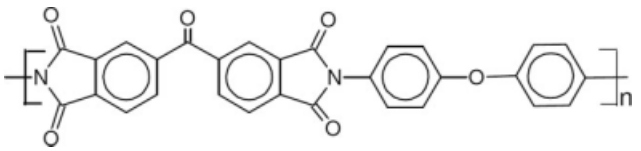

Figure 1 Chemical structure of PI foam derived from BTDA/4,4′-ODA.

EXPERIMENTAL

Materials

The BTDA was purchased from Shanghai Research Institute of Synthetic Resins, China, and used after drying at 150°C. The 4,4′-ODA was obtained from Bengbu Zuguang Finechem, China, and used as received. Tetrahydrofuran (THF) and methanol were supplied by Beijing Finechem, and used as blowing agent and the solvent.

Preparation of PI foam

4,4′-ODA was dissolved in mixture of THF and methanol at room temperature. To the stirring 4,4′-ODA solution, BTDA was added gradually and the mixture was stirred for 10–12 h to yield a homogenous precursor solution. The solution was then treated in vacuum oven at 70°C for 6–10 h. The resulting material was crushed into fine powder and separated by a sieve. The precursor fine powders were placed in an oven at 170°C for 10 min and inflated to form hollow microspheres. The hollow microspheres were placed into a mold. The mold was placed in air convection at 350°C for 2 h to obtain PI foam.

The glass transition temperature and limited oxygen index of this PI foam were 300°C and 65%, respectively.[7] Chemical structure of PI foam derived from BTDA/4,4′-ODA is shown in Figure 1.

Characterizations

Thermogravimetric analysis (TGA) was performed with NETZSCH STA TGA-409C at various heating rates in air and in nitrogen. The heating rates were 10, 20, 30, and 40°C/min, respectively. TG-FTIR studies were ramped from 25 to 800°C at 10°C/min. FTIR performed with Nicolet Nexus-670 was recorded in the spectral range of 4000 and 500 cm^{-1} with a resolution of 8 cm^{-1}.

RESULTS AND DISCUSSION

Analysis of TGA and TG-FTIR

TG curves of the PI foam at the various heating rates with 10, 20, 30, and 40°C/min in air and in nitrogen are shown in Figure 2(a,b). DTG curves of the PI foam at the various heating rates with 10, 20, 30, and 40°C/min in air and in nitrogen are shown in Figure 3(a,b).

In Figures 2 and 3, TG and DTG curves of the PI foam move toward high temperature with increasing heating rate. PI foam shows a remarkable weight decreasing in a narrow temperature range from 500 to 650°C in air and in nitrogen. PI foam degrades faster in air than in nitrogen, with ~ 55% residue remaining in nitrogen versus zero in air at 800°C. The temperature corresponding to the maximum decomposition occurring (T_{max}) of the PI foam can be easily determined from DTG curves. The 5% weight loss temperature ($T_{5\%}$), the 95% weight loss temperature ($T_{95\%}$), T_{max}, and weight remaining with the maximum decomposition occurring of the PI foam are given in Table I. The 5% weight loss temperature of the PI foam is lower in air than in nitrogen at the same heating rate. The residues remaining corresponding to the maximum decomposition occurring of the PI foam are about 85% in air and 54% in nitrogen, respectively.

Absorption strength of released gas (CO at 2183 cm^{-1}, CO_2 at 2352 cm^{-1}, H_2O at 3744 cm^{-1},

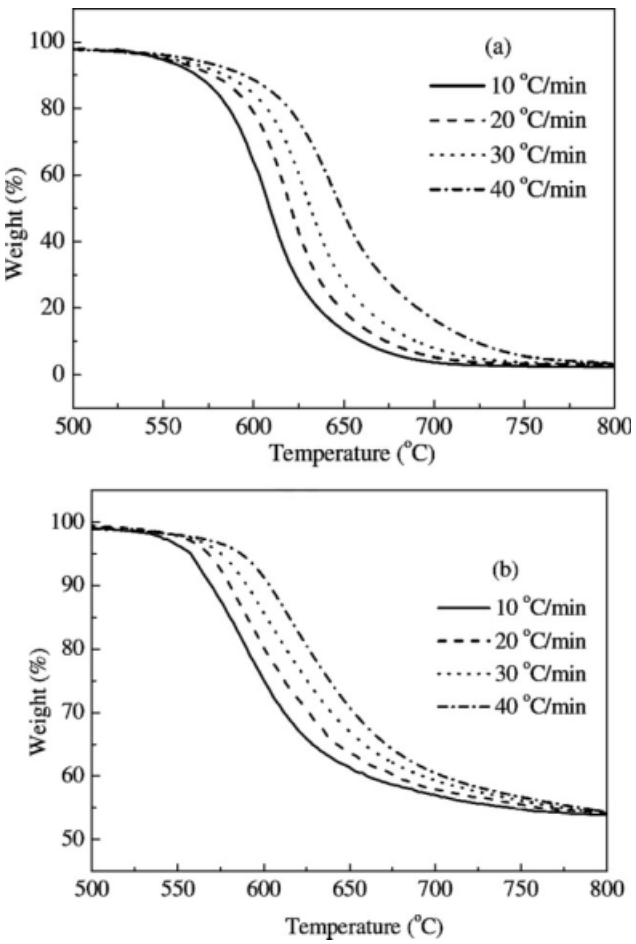

Figure 2 TG curves of PI foam: (a) in air; (b) in nitrogen.

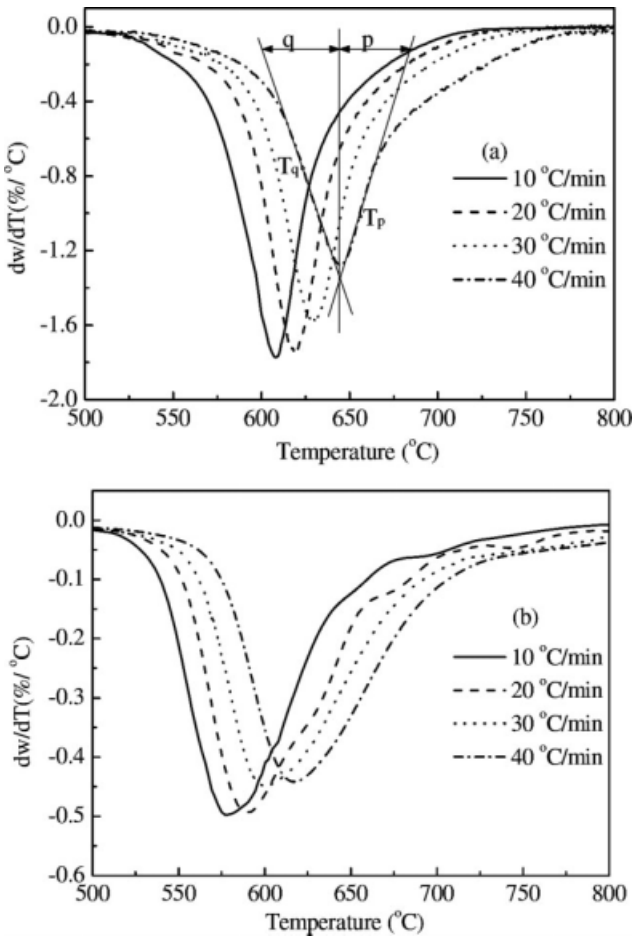

Figure 3 DTG curves of PI foam: (a) in air; (b) in nitrogen.

—N=C=O at 2285 cm^{-1}) versus heating time in air and in nitrogen are given in Figures 4 and 5, respectively. The intensities of general absorption peak, CO, CO_2, and H_2O absorption peak in air is stronger than in nitrogen, which shows that the decomposition gases are less in nitrogen than in air. The main gaseous decomposition products and decomposition temperatures of PI foam in air and in nitrogen are shown in Table II. Some representative FTIR spectra are shown in Figure 6 in air and Figure 7 in nitrogen.

The FTIR results show the evolution of CO_2, CO, and H_2O in air and CO_2, CO, H_2O, —N=C=O, CH_4, and —NH_2NH_2 in nitrogen. The stretching vibration of free O—H is in the range 3500–3800 cm^{-1}. The broad band above and below 1600 cm^{-1} is assigned to stretching vibration of H_2O and phenyl ring. The characteristic bands of CO_2 are at 2352 and 667 cm^{-1}. The characteristic double bands of CO are at 2183 and 2120 cm^{-1} at the right wing of the CO_2 band. The asymmetric stretching vibration of —N=C=O is at 2285 cm^{-1}. The vibration of CH_4 is at 3000 cm^{-1}. The characteristic double bands at 1000 cm^{-1} are assigned to —NH_2NH_2 vibration. Some diatomic molecules, such as hydrogen from benzene ring and nitrogen from imide ring, cannot be identified by infrared spectroscopy.

These results are consistent with mechanisms of thermal and thermal oxidative degradation of previously studied polyimide films, which indicates that CO, CO_2, and H_2O are the prevalent volatile products, with the imide ring as the site of initial degradation in air or inert atmosphere.[10–17] Both in air and in nitrogen, CO_2 evolved at low temperature is attributed to adsorbed or weakly bound species. At higher temperatures, the CO_2 has been attributed to decarboxylation of acid end groups and/or uncyclized amic acids, imide ring or anyhydride end-group hydrolysis followed by acid decarboxylation, thermal cleavage of the imide ring to yield an isocyanate with releasing of CO that dimerized yielding a carbodiimide and CO_2 or rearrangement of an imide to an isoimide, followed by thermal release of CO_2.[10,11] In nitrogen, the benzophenone in main chain is decomposed to biphenyl with the release of CO in the range from 500 to 700°C. The methane (CH_4), hydrogen, and nitrogen start to be released above 580°C, 600°C, and 800°C in nitrogen, respectively.[16]

Polyimide foam is known to degrade faster in air than in inert atmospheres. The water can lead to cleavage and decarboxylation of the imide ring and increases the rate of the degradation process. And at the same time, the imide ring can be oxidized to polymer peroxide or phenyl radical by oxygen in air. The decomposition reaction of PI foam is speeded up by water and oxygen in air.[10] Therefore, the 5% weight loss temperature of the PI foam is lower in air than in nitrogen at the same heating

TABLE I
Characteristic Temperature and Weight Remaining of Thermal Degradation for PI Foam

Heating rate (°C/min)	$T_{5\%}$ (°C)		T_{max} (°C)		Weight remaining at T_{max} (%)		$T_{95\%}$ (°C)	
	In air	In nitrogen	In air	In nitrogen	In air	In nitrogen	In air	In nitrogen
10	547	557	607	577	52	86	689	–
20	550	567	618	588	54	86	702	–
30	554	574	629	600	54	86	723	–
40	563	586	646	617	54	84	757	–

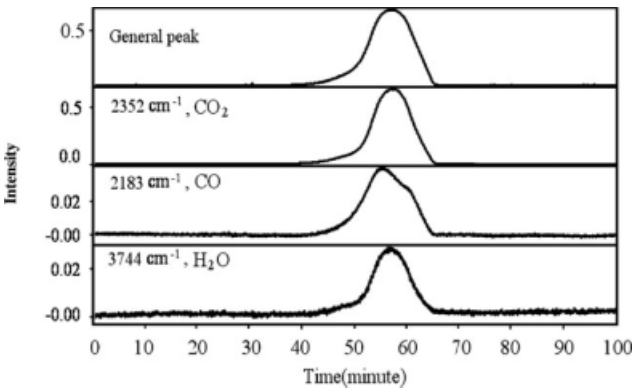

Figure 4 Changes of decomposition gases measured by FTIR spectra with heating treatment temperature in air.

rate. The main decomposed mechanism is shown in Figures 8 and 9.

In air, oxygen can not only react with PI to polymer peroxide or phenyl radical but react with primary decomposition products to CO, CO_2, and H_2O. Therefore, the residual mass is near to zero in air. There are about 55% residues in nitrogen at different heating rates. One of the expected degradation mechanisms for highly aromatic compounds such as the polyimide foam is crosslinking of the aromatic rings to form a pseudo-graphitic or charred carbonaceous material. It is reported in a thermogravimetric study of the thermal degradation of some polyimides that the degradation product of the pyrolyzed polyimide approaches that of graphite in inert atmosphere.[16–18]

Kinetic models

Various methods (integral, differential, and other special methods) are commonly used in the determination of the kinetic parameters. The Kissinger basic formula is[21]:

$$\frac{d}{dt}\left(\frac{d\alpha}{dt}\right) = \frac{d\alpha}{dt}\left[\frac{E\beta}{RT^2} - Ane^{-E/RT}(1-\alpha)^{n-1}\right] \quad (1)$$

where t is the heating time, α is the conversion rate, β is the heating rate, E and A are the so-called activation energy and pre-exponential factor (or frequency factor), n is the reaction order, and R is the general gas constant, respectively.

For $T = T_{max}$, equating $d^2\alpha/d^2t = 0$, the logarithm expression of (1) is:

$$\ln\left(\frac{\beta}{T_{max}^2}\right) = \ln\left[\left(\frac{AR}{E}\right)n(1-\alpha_{max})^{n-1}\right] - \frac{E}{RT_{max}} \quad (2)$$

The approximate expression of eq. (2) is:

$$\ln\left(\frac{\beta}{T_{max}^2}\right) = \ln\left(\frac{AR}{E}\right) - \frac{E}{RT_{max}} \quad (3)$$

Figure 10 shows the relationship of $\ln\frac{\beta}{T_{max}^2}$ and $\ln\frac{1}{T_{max}}$ in air and in nitrogen.

The multiple TGA curves are required by Kissinger method. It is possible to evaluate the activation energy from single TGA curve at the maximum rate of decomposition.[22–26] The analytical solution is:

$$E = nRT_{max}^2\frac{\left(\frac{d\alpha}{dT}\right)_{max}}{(1-\alpha_{max})} \qquad \forall n \quad (4)$$

The frequency factor can also be calculated from the thermal parameters determined at the peak temperature, activation energy, and heating rate, by means of the eq. (5):

$$A = \beta\frac{\left(\frac{d\alpha}{dT}\right)_{max}}{(1-\alpha_{max})^n}\exp\left(\frac{E}{RT_{max}}\right) \qquad \forall n \quad (5)$$

Assuming that the decomposition reaction is of first-order, the activation energies, the frequency factors, and regression coefficient (r^2) in air are listed in Table III.

Coats and Redfern equation for $n = 0$ is eq. (6).[27] The general analytical equation developed by Carrasco[23] is an infinite series. When the thermal energy (RT) is significantly less than activation energy (E), the sum can be truncated at the second term ($i = 2$). In this case, the kinetic equation is similar to that obtained by Coats and Redfern.

$$\ln\left[\frac{\alpha}{T^2}\right] = \ln\frac{AR}{\beta E} - \frac{E}{RT} \quad (6)$$

The differential method is[28]:

$$\ln\left[\frac{\left(\frac{d\alpha}{dT}\right)}{(1-\alpha)^n}\right] = \ln\left(\frac{A}{\beta}\right) - \frac{E}{RT} \quad (7)$$

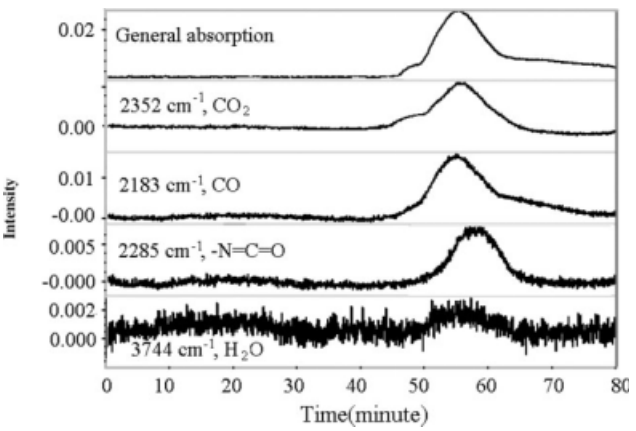

Figure 5 Changes of decomposition gases measured by FTIR spectra with heating treatment temperature in nitrogen.

TABLE II
The Main Gaseous Decomposition Products of PI Foam in Air and in Nitrogen

Gaseous decomposition product		T_i[a] (°C)		T_{max}[b] (°C)		T_f[c] (°C)	
In air	In nitrogen	In air	In nitrogen	In air	In nitrogen	In air	In nitrogen
CO	CO	451	460	578	573	672	–
CO_2	CO_2	436	445	603	585	655	728
H_2O	H_2O	452	–	592	–	676	–
–	—N=C=O	–	500	–	625	–	725
–	CH_4	–	580	–	–	–	–

[a] Initial releasing temperature of gaseous decomposition product.
[b] Maximum releasing temperature of gaseous decomposition product.
[c] Finished releasing temperature of gaseous decomposition product.

For the purpose of comparison, the results from the dynamic method and the analytical methods reported in the literature are summarized in Table III. As shown in Table III, there are some variations in the calculated kinetic parameters depending upon the mathematical approach taken in the analysis. These observations clearly indicate the problems in the selection and utilization of different analytical methods to solve the thermal degradation of polymers. Kissinger has shown that the product $n(1-\alpha)^{n-1} \approx 1$ is independent of the heating rate (β).The average energy calculated from eq. (4) is 199.4 kJ/mol in air. The method is not suitable to decomposition of PI foam in nitrogen due to inadequate decomposition of PI foam. The average energies calculated from eq. (6) are 207.4 kJ/mol in air and 243.7kJ/mol in nitrogen with assumed reaction order of zero. The energies calculated from eq. (7) are 306.3kJ/mol in air and 335.5kJ/mol in nitrogen. The determined activation energy for PI foam in air is lower than that in nitrogen, which shows that PI foam is easier to decompose in air than in nitrogen. The same trends are found in the pre-exponential factors calculated by different methods. The reaction energies and pre-exponential factors calculated from Kissinger method, eq. (6) and Coats and Redfern method are similar.

The decomposition reaction order of polymer is usually considered as first order for simplifying model and convenient calculation. But the pyrolysis process of polymer is very complex and changes with atmosphere.

The reaction order can be calculated from Crane equation[29]:

$$\frac{d\ln\beta}{d(1/T_{max})} = -\frac{E}{nR} - 2T_{max} \tag{8}$$

The reaction order can be obtained from slope with different E values. The degradation reactions of PI foam in air and in nitrogen are both near to a first-order reaction calculated by Crane and Kissinger and eq. (4). The average reaction orders determined by Crane and Coats and Redfern method are

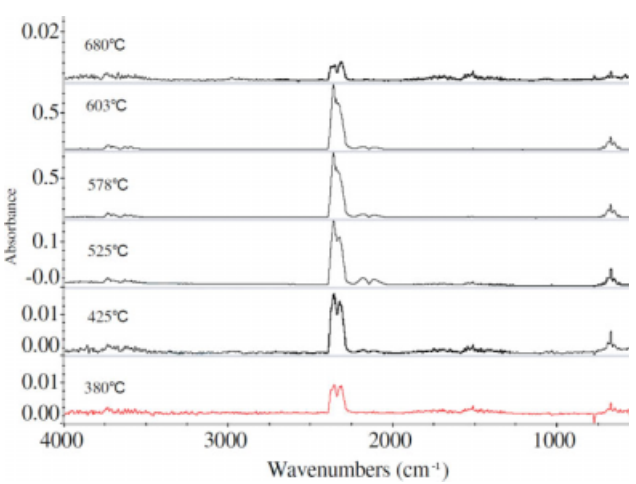

Figure 6 Stacked FTIR spectra for the decomposition products of PI foam in air. [Color figure can be viewed in the online issue, which is available at www.interscience.wiley.com.]

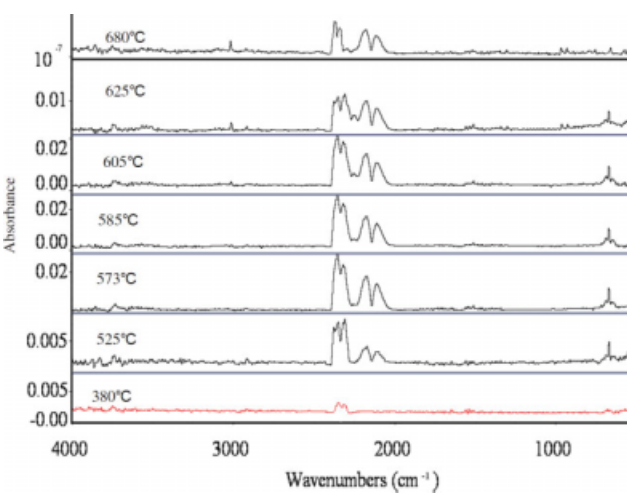

Figure 7 Stacked FTIR spectra for the decompositon products of PI foam in nitrogen. [Color figure can be viewed in the online issue, which is available at www.interscience.wiley.com.]

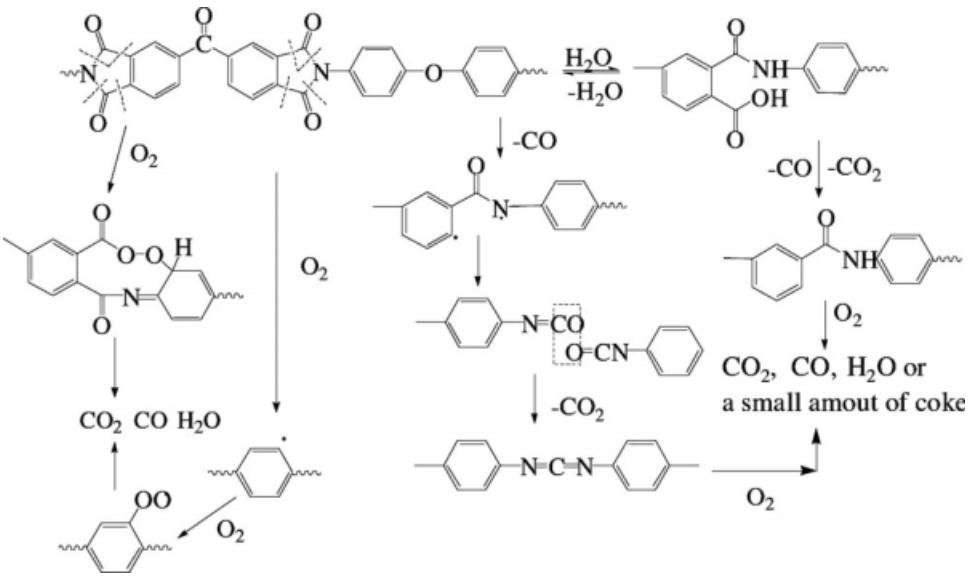

Figure 8 The possible decomposition mechanism of PI foam in air.

1.1 in air and 1.2 in nitrogen, respectively. The average reaction orders calculated by Crane and differential method are near to 1.6.

Kissinger proposed a shape index semi-empirical equation to calculate reaction order from the differential thermal analysis data. This equation is convenient for the estimation of reaction order. To quantitatively describe the peak shape a "shape index" is proposed, defined as the absolute value of the ratio of the slopes of tangents to the curve at the inflection points. This shape index is illustrated in Figure 3(a). Shape index (S) can be calculated from DTG curves and $S = p/q$. It can be expressed analytically as[21]:

$$S = \frac{\left(\frac{d^2\alpha}{dT^2}\right)_{Tq}}{\left(\frac{d^2\alpha}{dT^2}\right)_{Tp}} \tag{9}$$

where subscript T_q and T_p refer to the temperatures at the inflection points from the second derivative TG (2DTG) curve.

The relationship between reaction order and shape index can be expressed as the following function:

$$n = 1.26S^{\frac{1}{2}} \tag{10}$$

The reaction order n is different for each curve. Shape indexes, temperatures at inflection points (T_q

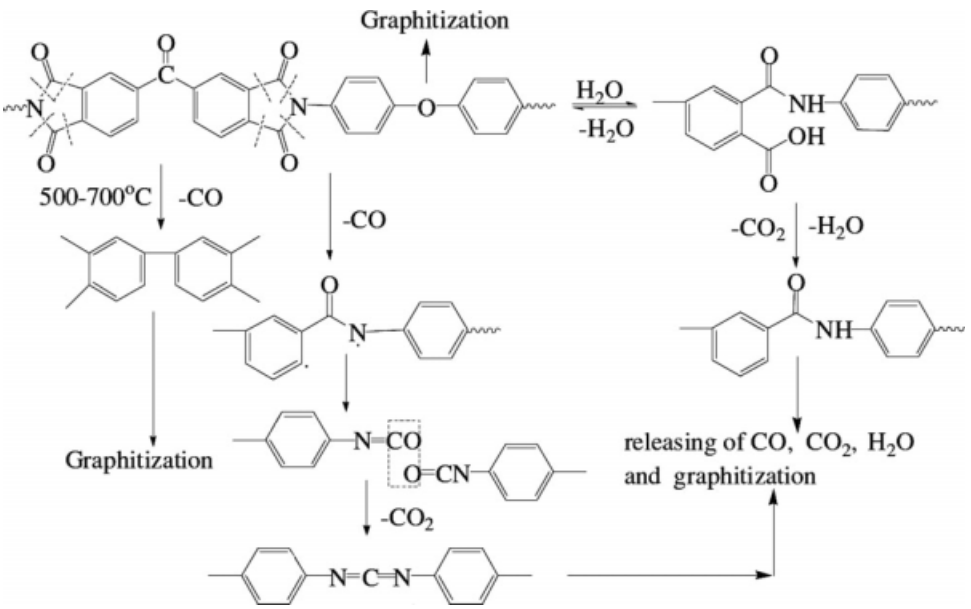

Figure 9 The possible decomposition mechanism of PI foam in nitrogen.

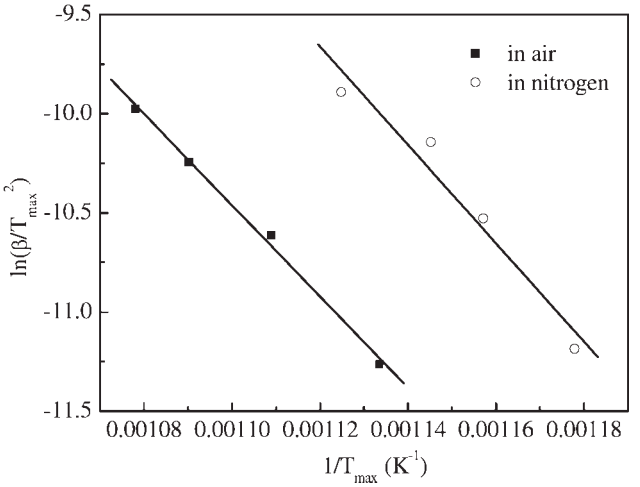

Figure 10 Kinetics analysis of PI foam by Kissinger method.

and T_p), the second derivative values, and reaction orders at different heating rates are shown in Table IV. The average reaction orders of decomposition reaction for PI foam in air and in nitrogen are equal to 1.2 and 1.8, respectively.

But the order determined by such an index is rough and approximate. The shape index method proposed by Kissinger has been considered that $E/RT = \infty$ and neglecting the influence of the peak width or heating rate on the S value.[30] In general, the ultimate reaction order is an average value of reaction orders at different heating rates.[21,31–33]

The oxygen and water in air can accelerate degradation of PI foam until complete decomposition of PI foam, which possibly results in that q value at lower temperature is near to p value at the higher temperature. In nitrogen, decomposition reaction rate of PI foam decrease at the higher temperatures due to carbonization, which shows that p value is higher than q value in DTG curve. Therefore, the n values calculated in air are lower than in nitrogen.

The reaction order calculated by Crane is proportional to activation energy. The determined activation energy in air is lower than that in nitrogen. Whatever Crane or Kissinger method, the reaction orders in nitrogen are higher than those in air. It indicates that the released gas concentration has greater influence on the decomposition reaction rate in nitrogen than in air.

CONCLUSIONS

1. TG and DTG curves of PI foam derived from BTDA/4,4′-ODA move toward high temperature with increasing heating rate. The 5% weight loss temperature is higher in air than in

TABLE III
The Decomposition Kinetic Parameters of PI Foam

Method	E (kJ/mol)	A (s^{-1})	r^2	N	
				Assumed method	Crane method
Kissinger					
In air	191.5	1.11×10^{9}	0.9958	1.0	1.0
In nitrogen	206.4	3.13×10^{10}	0.9541	1.0	1.0
The general analytical equation					
10°C/min (in air)	220.4	6.66×10^{12}	–	1.0	1.1
20°C/min (in air)	212.7	3.17×10^{10}	–	1.0	1.1
30°C/min (in air)	198.2	4.40×10^{9}	–	1.0	1.0
40°C/min (in air)	166.4	8.99×10^{7}	–	1.0	0.9
Coats and Redfern					
10°C/min (in air)	211.5	8.93×10^{9}	0.9966	0.0	1.1
20°C/min (in air)	230.9	1.76×10^{11}	0.9930	0.0	1.2
30°C/min (in air)	204.9	4.88×10^{9}	0.9926	0.0	1.1
40°C/min (in air)	182.4	1.82×10^{8}	0.9958	0.0	1.0
10°C/min (in nitrogen)	259.1	8.12×10^{12}	0.9940	0.0	1.3
20°C/min (in nitrogen)	262.7	1.61×10^{13}	0.9942	0.0	1.3
30°C/min (in nitrogen)	234.3	3.06×10^{11}	0.9972	0.0	1.1
40°C/min (in nitrogen)	218.8	2.87×10^{10}	0.9966	0.0	1.1
Differential method					
10°C/min (in air)	291.4	8.78×10^{14}	0.9924	1.0	1.5
20°C/min (in air)	307.8	7.33×10^{15}	0.9886	1.0	1.6
30°C/min (in air)	342.9	2.03×10^{18}	0.9938	1.0	1.8
40°C/min (in air)	283.2	2.03×10^{14}	0.9956	1.0	1.5
10°C/min (in nitrogen)	368.7	7.61×10^{19}	0.9936	1.0	1.8
20°C/min (in nitrogen)	322.4	9.68×10^{16}	0.9902	1.0	1.6
30°C/min (in nitrogen)	326.1	1.37×10^{17}	0.9944	1.0	1.6
40°C/min (in nitrogen)	325.0	6.98×10^{16}	0.9900	1.0	1.6

TABLE IV
The Shape Parameters at Different Heating Rates

Heating rate (°C/min)	Atmosphere	T_q (°C)	T_p (°C)	$(d^2\alpha/dT^2)_q$	$(d^2\alpha/dT^2)_p$	S	n
10	In air	598	618	5.33×10^{-4}	-6.42×10^{-4}	0.83	1.15
10	In nitrogen	556	618	1.41×10^{-4}	-7.71×10^{-5}	1.83	1.70
20	In air	607	629	6.20×10^{-4}	-6.22×10^{-4}	1.00	1.26
20	In nitrogen	564	629	1.39×10^{-4}	-5.84×10^{-5}	2.38	1.94
30	In air	616	641	4.99×10^{-4}	-5.06×10^{-4}	0.99	1.25
30	In nitrogen	582	636	1.34×10^{-4}	-6.14×10^{-5}	2.18	1.86
40	In air	624	656	3.22×10^{-4}	-3.54×10^{-4}	0.91	1.20
40	In nitrogen	592	658	1.19×10^{-4}	-5.53×10^{-5}	2.15	1.85

nitrogen at the same heating rate. PI foam degrades faster and is less stable in air than in nitrogen. The residues in nitrogen at 800°C are approximate to 55% versus zero in air.

2. The main pyrolysis products of PI foam are CO_2, CO, and H_2O in air, which shows that PI foam derived from BTDA/4,4′-ODA is an environmentally friendly material. It should be noted that there are some small organic molecules and graphitized solid residues in the pyrolysis products of PI foam in nitrogen.
3. The mathematical treatments of the experimental data using different analytical models produce different results, which are due to the different approximation techniques used in deriving these models. From the kinetic parameters calcualated by kinetic models reported in the literature, it is found that the activation energies and frequency factors of PI foam are higher in nitrogen than in air. The reaction orders calculated by Crane method increase with the increasing activation energies. The decomposition reaction order of PI foam in air is higher than that in nitrogen.

References

1. Dai, Z.; Li, Y. F.; Yang, S. G.; Zhan, N.; Zhang, X. L.; Xu, J. Eur Polym J 2009, 45, 1941.
2. Thirumal, M.; Khastgir, D.; Singha, N. K.; Manjunath, B. S.; Naik, Y. P. J Appl Polym Sci 2008, 110, 2586.
3. Mao, Y. P.; Qi, R. R. J Appl Polym Sci 2008, 109, 3249.
4. Farrissey, W. J., Jr.; Rose, J. S.; Carleton, P. S. J Appl Polym Sci 1970, 14, 1093.
5. Chu, H. J.; Zhu, B. K.; Xu, Y. Y. J Appl Polym Sci 2006, 102, 1734.
6. Vazquez, J. M.; Cano, R. J.; Jensen, B. J.; Weiser, E. S. U.S. Pat. 7,541,388 (2009).
7. Shen, Y. X.; Zhan, M. S.; Wang, K. Polym Adv Technol, to appear.
8. Hshieh, F. Y.; Hirsch, H. B.; Beeson, H. D. Fire Mater 2003, 27, 119.
9. Williams, M. K.; Holland, D. B.; Melendez, O.; Weiser, E. S.; Brenner, J. R.; Nelson, G. L. Polym Degrad Stab 2005, 88, 20.
10. Kuroda, S. I.; Mita, I. Eur Polym J 1989, 25, 611.
11. Cella, J. A. Polym Degrad Stab 1992, 36, 99.
12. Tiptipakorn, S.; Damrongsakkul, S.; Ando, S.; Hemvichian, K.; Rimdusit, S. Polym Degrad Stab 2007, 92, 1265.
13. Chou, W. J.; Wang, C. C.; Chen, C. Y. Polym Degrad Stab 2008, 93, 745.
14. Meng, X. L.; Huang, Y. D.; Yu, H.; Lv, Z. S. Polym Degrad Stab 2007, 92, 962.
15. Ren, L.; Fu, W. W.; Luo, Y. F.; Lu, H.; Jia, D. M.; Shen, J. R.; Pang, B.; Ko, T. M. J Appl Polym Sci 2004, 91, 2295.
16. Inagaki, M.; Ibuku, T.; Takeichi, T. J Appl Polym Sci 1992, 44, 521.
17. Lua, A. C.; Su, J. Polym Degrad Stab 2006, 91, 144.
18. Zhao, S.; Shi, Z. Q.; Wang, C. Y.; Chen, M. M. J Appl Polym Sci 2008, 108, 1852.
19. Williams, M. K.; Weiser, E. S.; Fesmire, J. E.; Grimsley, B. W.; Smith, T. M.; Brenner, J. R.; Nelson, G. L. Polym Adv Technol 2005, 16, 167.
20. Weiser, E. S.; Johnson, T. F.; St Clair, T. L.; Echigo, Y.; Kaneshiro, H.; Grimsley, B. W. High Perform Polym 2000, 12, 1.
21. Kissinger, H. E. Anal Chem 1957, 19, 1702.
22. Heitz, M.; Carrasco, F.; Chornet, E.; Overend, R. P. Thermochim Acta 1989, 142, 83.
23. Carrasco, F. Thermochim Acta 1993, 213, 115.
24. Carrasco, F.; Pagès, P. J Appl Polym Sci 2004, 93, 1913.
25. Carrasco, F.; Dionisi, D.; Martinelliy, A.; Majone, M. J Appl Polym Sci 2006, 100, 2111.
26. Carrasco, F.; Pagès, P. Polym Degrad Stab 2008, 93, 1000.
27. Coats, A. W.; Redfern, J. P. Nature 1964, 201, 68.
28. Bagchi, T. P.; Sen, P. K. Thermochim Acta 1981, 51, 175.
29. Crane, L. W.; Dynes, P. J.; Kaelble, D. H. J Polym Sci Part C: Lett 1973, 11, 533.
30. Llópiz, J.; Romero, M. M.; Jerez, A.; Laureiro, Y. Thermochim Acta 1995, 256, 205.
31. Park, P.; Kamal, K. K. Mater Chem Phys 2009, 113, 953.
32. Gao, C. C.; Li, X. G.; Feng, L. J.; Xiang, Z. C.; Zhang, D. H. Chem Eng J 2009, 150, 551.
33. Paik, P.; Kar, K. K. Polym Degrad Stab 2008, 93, 24.